

UCLA

UCLA Previously Published Works

Title

Phase Locking of a THz QC-VECSEL to a Microwave Reference

Permalink

<https://escholarship.org/uc/item/0nb9b8wz>

Journal

IEEE Transactions on Terahertz Science and Technology, 13(5)

ISSN

2156-342X

Authors

Curwen, Christopher A

Kawamura, Jonathan H

Hayton, Darren J

et al.

Publication Date

2023

DOI

10.1109/tthz.2023.3280451

Peer reviewed

Phase locking of a THz QC-VECSEL to a microwave reference

Christopher A. Curwen, Jonathan H. Kawamura, Darren J. Hayton, Sadvikas J. Addamane, John L. Reno, Benjamin S. Williams, and Boris S. Karasik

Abstract—High resolution frequency study and phase-locking have been performed on a terahertz quantum-cascade vertical-external-cavity surface-emitting-laser operating around 2.5 THz. A subharmonic diode mixer is used to down convert the THz signal to a 100 MHz intermediate frequency that is phase locked to a stable 100 MHz microwave reference. Between 90-95% of the QC-VECSEL signal is locked within 2 Hz of the multiplied RF reference, and amplitude fluctuations on the order of 1-10% are observed, depending on the bias point of the QC-VECSEL. The bandwidth of the locking loop is ~1 MHz. Many noise peaks in the IF signal are observed, likely corresponding to mechanical resonances in the 10 Hz-10 kHz. These peaks are generally -30 to -60 dB below the main tone, and are below the phase noise level of the multiplied RF reference which ultimately limits the phase noise of the locked QC-VECSEL.

Index Terms— Terahertz metamaterials, quantum cascade lasers, surface emitting lasers, laser stability, laser noise, phase locked loops.

I. INTRODUCTION

TERAHERTZ (THz) quantum-cascade lasers (QCLs) are a leading candidate for providing high power (milliwatt level) coherent THz radiation from a compact, electrically driven semiconductor source [1]. As the THz frequency range is rich in atomic and molecular rotational and vibrational resonances, THz QCLs can be essential tools for building THz spectroscopy systems [2, 3]. They are also of particular interest as local oscillators for astrophysical heterodyne receivers. However, a number of performance challenges must be addressed for THz QCLs to be effective sources for spectroscopy, such as frequency stability, frequency tunability, and beam quality. While frequency

stability is a common issue for semiconductor lasers, issues of beam quality and frequency tunability are particularly acute for THz QCLs due to the subwavelength thickness of metal-metal waveguide resonators typically used [4]. Such subwavelength facets result in poor, diffracted output beams, and also makes it difficult to couple external signals into the device, reducing the effectiveness of external cavity configurations that are typically used to tune the lasing frequency over broad bandwidths [5, 6]. Such facet coupling efficiency can be improved with use of a surface-plasmon (SP) waveguides [7], however the coupling is still far from ideal, and SP waveguides require lower operating temperatures due to higher losses and reduced confinement of the THz mode to the QC gain material.

One approach that can address many of the challenges facing THz QCL performance is the THz QC vertical-external-cavity surface-emitting-laser (VECSEL) [8, 9]. The QC-VECSEL is based on an amplifying metasurface reflector that, when combined with an external feedback mirror, forms an external cavity laser. Because the metasurface has a large surface-radiating area (millimeter scale), it couples efficiently to fundamental Gaussian modes of the external cavity, resulting in a high-quality output beam. Additionally, the lasing frequency is determined by the length of the external cavity, which can be mechanically tuned over broad bandwidths [10, 11]. One remaining aspect that we investigate in this study is the frequency stability and phase-locking of the QC-VECSEL.

Frequency- and phase- locking of ridge waveguide THz QCLs has been demonstrated using a variety of techniques including: referencing the QCL to a more stable gas laser or frequency multiplier chain (FMC) source using a superconducting hot electron bolometer [12, 13] or diode mixer [14, 15], locking to an optical or THz frequency comb [16-18], locking to a subharmonic diode mixer with an RF synthesized pump [19, 20], direct injection locking with signal from a THz photomixer [21], and locking to a molecular absorption line [22-24].

In this paper, we report the stabilization of a THz QC-VECSEL by phase locking it to a microwave reference using a subharmonic Schottky diode mixer. While this technique was previously reported [19, 20], the external cavity nature of the QC-VECSEL likely makes it more susceptible to external mechanical noise sources that are not present in ridge waveguide devices. Additionally, the electronic frequency tuning behavior is different from that of a ridge waveguide, which prompts a call for a dedicated study (see Appendix).

This research study was carried out, in part, at the Jet Propulsion Laboratory, California Institute of Technology, under a contract with the National Aeronautics and Space Administration. This work was supported, in part, by the National Science Foundation (1711892, 2041165), and the National Aeronautics and Space Administration (NNX16AC73G, 80NSSC19K0700). (*Corresponding author: Christopher A. Curwen*).

Christopher A. Curwen, Jonathan H. Kawamura, Darren J. Hayton, and Boris S. Karasik are with the Jet Propulsion Laboratory, California Institute of Technology, Pasadena, CA 91109 USA (e-mail chris.a.curwen@jpl.nasa.gov; jonathan.h.kawamura@jpl.nasa.gov; darren.j.hayton@jpl.nasa.gov; boris.s.karasik@jpl.nasa.gov)

Sadvikas J. Addamane and John L. Reno are with the Center for Integrated Nanotechnologies at Sandia National Laboratories, Albuquerque, NM 87185 USA (e-mail: saddamane@sandia.gov ; jreno@sandia.gov).

Benjamin S. Williams is with the Department of Electrical and Computer Engineering at the University of California, Los Angeles, CA 90095 USA (e-mail: bswilliams@ucla.edu).

Color versions of one or more of the figures in this article are available online at <http://ieeexplore.ieee.org>

II. METHODS

QC-VECSEL design and characterization

The design and operating principles of the QC-VECSEL are illustrated in Figs. 1(a) and (b). At the heart of the design is an amplifying reflectarray metasurface that consists of subwavelength metal-metal ridge-waveguide antennas resonantly coupled to surface radiation. The ridges are loaded with THz QC gain material such that incident radiation couples to the gain material via the waveguide antennas and is amplified before radiating back out in the reflected direction. Finite-element simulations of the reflection amplitude and phase of the metasurface tested in this work are plotted in Fig. 1(a). An insulating silicon dioxide layer is used between the top metal and semiconductor to selectively bias the center of the metasurface. When an external mirror is added (inset of Fig. 1(b)), the QC-VECSEL lases on the cavity mode with lowest diffraction loss, i.e. a fundamental Gaussian mode (assuming a perfect cavity).

The metasurface design has an $85 \mu\text{m}$ period and $16.35 \mu\text{m}$ wide ridges and used a hybrid bound-to-continuum/resonant-phonon active region design [25] (exact layer sequence can be found in [26]). The active region is only $5 \mu\text{m}$ thick (compared to the typical $10 \mu\text{m}$) in order to improved heat sinking during continuous wave operation [26]. The metasurface has a total area of $2 \times 2 \text{ mm}^2$, but only a central circular area 0.8 mm in diameter is biased. Additionally, the widths of the ridges are spatially varying to create a focusing phase profile with a focal length of 7 mm [27]. The metasurface was mounted with a fixed-length VECSEL cavity. The output coupler consists of a mesh of $3 \mu\text{m}$ wide metal lines deposited at a $15 \mu\text{m}$ pitch on a $200 \mu\text{m}$ thick z-cut crystal quartz substrate. The output coupler transmission was $\sim 12\%$ at 2.5 THz . The QC-VECSEL cavity was $\sim 450 \mu\text{m}$ long and lasing occurred at 2.51 THz . The current, voltage, and output power data for the QC-VECSEL are plotted in Fig. 1(b). The device is operated in continuous wave and outputs $\sim 1.2 \text{ mW}$ of THz power at a heat sink temperature of 77 K (measured outside the cryostat with a 90% transmissive cryostat window).

Experimental Setup

The experimental setup is illustrated in Fig. 2(a). A subharmonic diode mixer is used to down convert the QC-VECSEL signal to an intermediate RF frequency that can then be phase locked to an RF reference source. This strategy has been demonstrated in [19, 20, 28]. Here, we start with a $\sim 11 \text{ GHz}$ signal generator (Agilent E8257D), followed by a Spacek Labs tripling amplifier (A345-3XW-31), followed by a JPL-made passive tripler. This local oscillator (LO) chain can generate $>100 \text{ mW}$ at $\sim 100 \text{ GHz}$, but only $\sim 8 \text{ mW}$ are needed to pump the subharmonic mixer. The 2.5 THz QCL signal mixes with the 25^{th} harmonic of the LO. The mixer is a modified version of the device described in [20]. The QC-VECSEL beam is focused via an HDPE lens into the mixer's diagonal feed horn antenna. The IF signal is set to $\sim 3 \text{ GHz}$, amplified by 60 dB , filtered through a 500 MHz wide

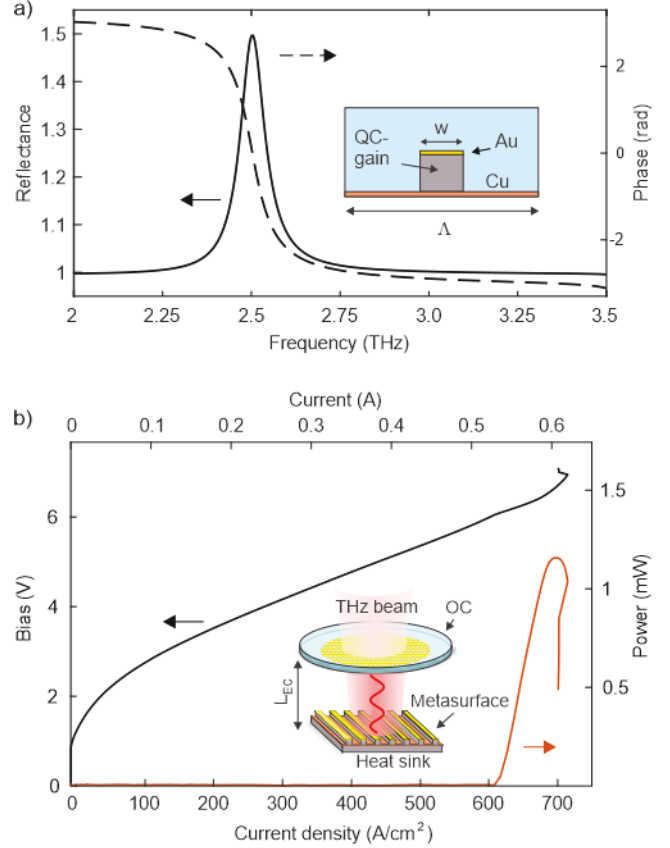


Fig. 1. (a) FEM simulated magnitude and phase of the metasurface reflectance with 20 cm^{-1} gain applied to the QC material. Metasurface structure is illustrated in the inset. (b) Measured lasing characteristics of the resulting QC-VECSEL, illustrated in inset.

bandpass filter, down-converted to 100 MHz with a second mixer (Mini-circuits ZEM-4300+), and sent to the phase-lock loop (PLL) electronics (XL Microwave 800A). The PLL uses the bias on the QC-VECSEL as a frequency/phase tuning mechanism to correct for any difference in phase between the reference and IF signals. The bandwidth of the PLL is $\sim 1 \text{ MHz}$. The IF signal is monitored with a -10 dB coupler and a Keysight PXA signal analyzer. The down-conversion is performed in two steps because the PLL requires an IF frequency around 100 MHz , but the THz subharmonic mixer has significant IF noise in the vicinity of 100 MHz . The output of the PLL provides both the DC bias and the superimposed error correction. The output of the PLL is also monitored on an oscilloscope. We observe a conversion loss of $\sim 100 \text{ dB}$.

IV. RESULTS

We first measure the free-running absolute frequency and frequency stability of the QC-VECSELs with the phase-lock loop off. The results are plotted in Fig. 2(b) as a function of device bias. Total frequency tuning across the dynamic range of the device is $\sim 1 \text{ GHz}$. The high-resolution spectrum of the THz signal is measured via the IF on the signal analyzer. The non-linear frequency tuning characteristic with bias is related to external feedback from the mixer (17 cm distance), and is well modeled by a Lang-Kobayashi feedback model [29]. If single millisecond scans are collected, a narrow spectral line

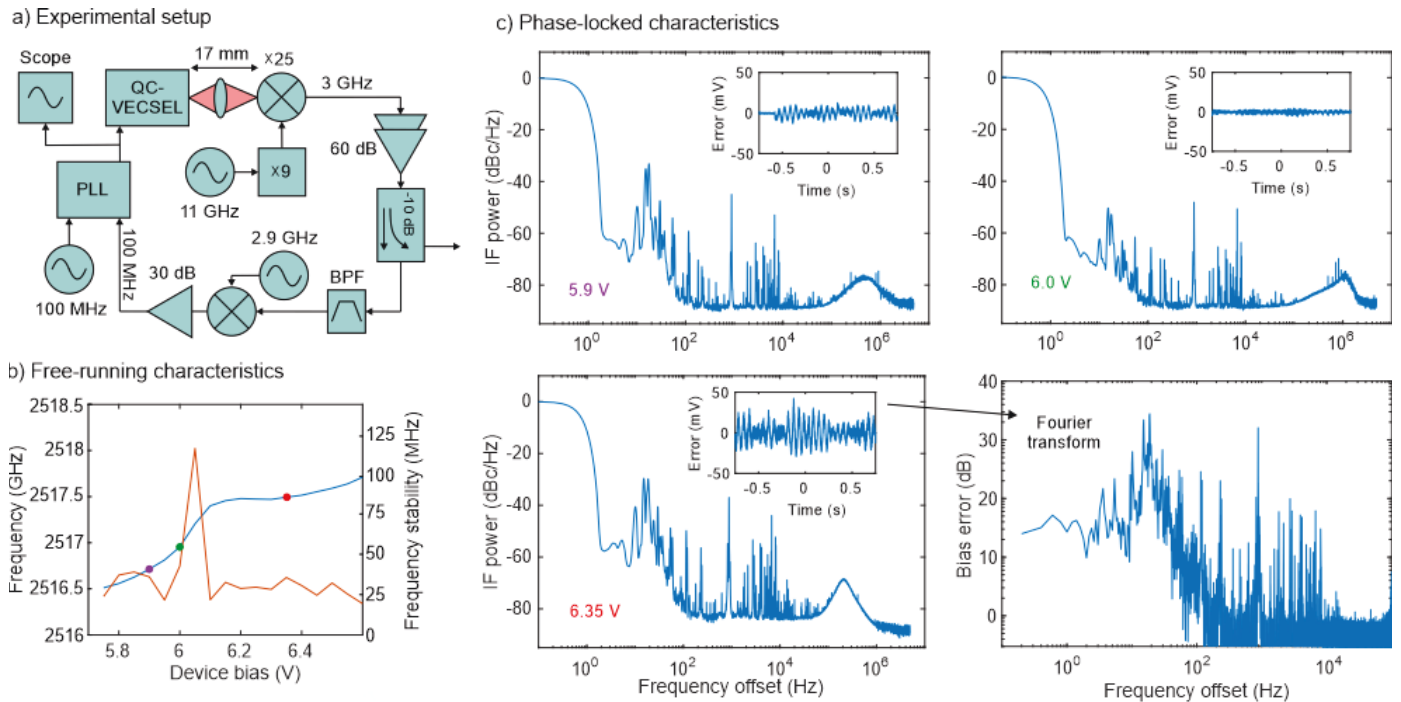


Fig. 2. (a) Block diagram of down conversion and phase-locking of the THz QC-VECSEL. (b) Measured lasing frequency and frequency stability as a function of bias. (c) Measured IF power with the phase-lock loop on. Insets time-domain measurement of bias fluctuations on the device, which are proportional to the error signal from the locking electronics. Fourier transform of the bias signal is plotted in the bottom right.

(limited by the resolution bandwidth of the observation) is observed that jumps-around on each sweep. The frequency stability is characterized by using the signal analyzer to perform max-hold measurements of the IF signal over the course of 5 seconds, capturing the maximum extent of the QC-VECSEL frequency jitter during the measurement time. The span of this jitter is plotted as frequency stability in Fig. 2(b), and is observed to be 25-50 MHz on average. We note that slow drifts in the VECSEL frequency are not captured in these measurements; the measured frequency jitter is the same whether hold time is tens of milliseconds or tens of seconds. Slow drifts are observed on the scale of minutes or hours, but not on the scale of the max-hold data recording time. For comparison, typical frequency jitter for ridge waveguide THz QCLs tend to be narrower, in the 1-10 MHz range [12, 15, 30, 31]. Utilizing a more rigid external cavity or a more stable bias supply was not observed to improve the frequency stability of the VECSEL, suggesting that the source of noise may be unstable feedback from optics in the setup.

In Figure 2(c), the single-sideband IF power spectrum while phase locking the QC-VECSEL is plotted for several different bias points. More than 95% of the power is contained within 2 Hz of the RF reference at all bias points (ratio of integrated IF power in a 2 Hz bandwidth and integrated power within the bandwidth of the PLL), and most of the unlocked power is in broad peaks around 1 MHz associated with the bandwidth of the PLL. It is observed that there are many noise peaks in the locked IF spectrum in the range of ~ 10 Hz – 10 kHz, which we assume to be associated with mechanical noise in the system, perhaps affecting the feedback. As the device is phase-locked, these peaks should correspond to amplitude

noise, which is confirmed by measurement of error signal fed into the device bias while phase-locked (insets in plots in Fig. 2(c)). Fourier transform of the bias fluctuations matches well with the measured IF spectrum.

It is observed that the phase noise is significantly larger at certain bias points where the frequency tuning coefficient with bias is small (ex. 6.25 V versus 6.0 V), and smaller where the tuning coefficient is large (6.0 V). This is because the larger tuning coefficient allows a given frequency error to be corrected with a smaller change in device bias and output power. This is confirmed by observation that the error signal has peak-to-peak fluctuations on the order of 10 mV when biased at 6.0 V, and peak fluctuations of 100 mV when biased at 6.35 V, which corresponds to ~ 1 and 10% power variations, respectively. However, the noise peaks at higher kHz frequencies are not noticeably impacted by the device bias point. This is likely because the tuning curve in Fig. 2(b) is measured over a long timescale and is the combined result of thermal and electrical tuning. At lower frequencies, this curve applies, but at higher frequencies, only the electrical tuning response is present, which is apparently a more constant as function of bias. We note that the device could not be phase-locked in a small range of bias around 6.3 V, where the direction of the tuning coefficient briefly switches polarity, making the tuning coefficient non-monotonic. Such an issue was also observed in [32].

In Fig. 3, we use a second subharmonic diode mixer to observe the QC-VECSEL signal while still phase-locked by the first mixer. The second mixer operates on the 3rd harmonic of an 833 GHz LO [33]. The synthesizers used at the start of

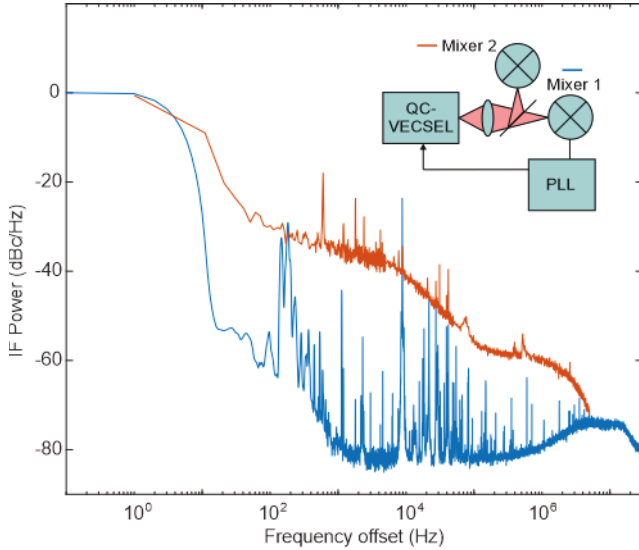


Fig. 3. Phase noise comparison between locking mixer (mixture 1, blue) and observing mixer (mixture 2, red).

LO chains for the two mixers are synchronized. The phase noise is much larger according to the second observing mixer, and is in good agreement with the expected stability of the multiplied-up reference which experiences a degradation in phase noise according to $20 \log_{10}(N)$, where N is the multiplication factor. A similar effect is observed when locking with the second mixer [34] and observing with the first. Therefore, it is demonstrated that the true phase-noise of the locked VECSEL is limited by that of the reference.

Last, for comparison, we tested a second, 3.4 THz QC-VECSEL (same as device in [10]) in a second, more mechanically rigid dewar (Kadel KR373 versus IRLabs ND-3). The metasurface is mounted in a fixed-length VECSEL cavity, same as the 2.5 THz device. The phase-locked IF power spectrum of the second QC-VECSEL is plotted in Fig. 4. It is observed that all peaks in noise below 1 kHz are nearly extinguished, and the higher frequency noise is reduced, but some noteworthy peaks are still present. This improvement is indicative that vibration of the dewar may be the primary source of noise / frequency instability.

VIII. CONCLUSIONS

In this paper, we have used a subharmonic diode mixer driven by a microwave synthesized LO to study the high-resolution frequency behavior and phase-locking of a THz QC-VECSEL. The free-running linewidths are found to be in the tens of MHz, and phase locked linewidths of <1 Hz are achieved. There are remaining noise peaks in the 10 Hz – 10 kHz frequency range resulting from amplitude fluctuations in the phase-locked device (a side effect of using the bias on the device as the mechanism of frequency and phase control). These noise peaks are 40-60 dB below the main tone, which is lower than the phase noise of the multiplied microwave reference, making them a non-issue with regards to spectral resolution, but the amplitude fluctuations increase the averaging time necessary to measure small signals and would limit the sensitivity of a measurement assuming a given Allan variance time for the system. Amplitude stabilization

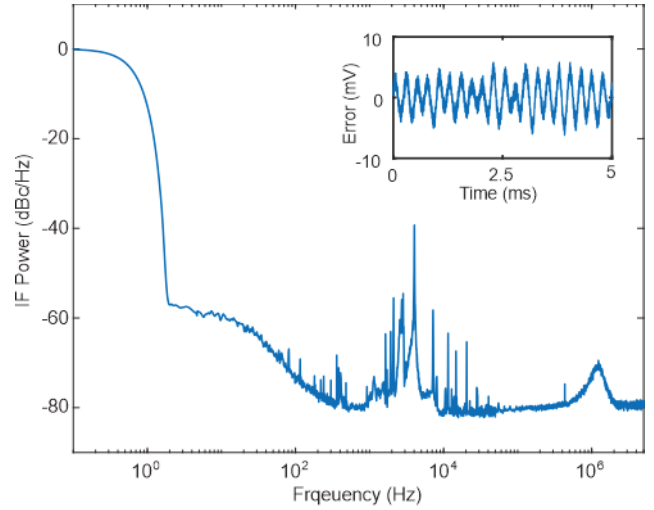


Fig. 4. Reduced phase noise of QC-VECSEL mounted in more mechanically rigid dewar.

of QCLs has been demonstrated using a number of external components, such as a tunable beam block controlled with a voice coil [35], injecting power from an infrared laser into the QCL substrate to tune the refractive index via excitation of electron-hole pairs [36], and using a graphene based split-ring resonator metasurface [37]. These approaches may be adaptable to the VECSEL, depending on the actuation speeds (particularly for a beam block) and potential coupling to frequency tuning, resulting in a more complex coupled system. An intriguing alternate approach may be to phase-lock the QC-VECSEL using piezoelectric control of cavity length as the error correction mechanism, rather than the bias on the metasurface. The cavity only needs to be tuned by nanometers to correct for the frequency error, and piezoelectric stack actuators have demonstrated actuation frequencies as high as 500 kHz [38]. The output coupler transmission changes very little ($<0.01\%$) on the MHz scale tuning needed to phase lock the device, so this should provide a mechanism for nearly pure frequency modulation, which will obviate the need for additional amplitude stabilization. Finally, we suggest that due to its large emitting aperture, the VECSEL is likely amenable to direct injection locking with a low-power, stable tone from a THz photomixer [21] or diode frequency multiplier. Such a scheme should lock the phases of the sources without inducing amplitude fluctuations. However, the power from these sources is extremely small at higher THz frequencies, and the signal must be coupled in through a low reflectance beam splitter because the QC-VECSEL only outputs power from one side (unlike a ridge waveguide that can be injected from the back facet and output from the front facet), which may make it difficult to inject sufficient power for locking. Such strategies and improvements will be investigated in continued studies.

APPENDIX: QC-VECSEL TUNING COEFFICIENTS

For the QC-VECSEL, the round-trip phase accumulation when lasing is given by $2kL_{ext} - \phi_{MS}(n) - \phi_{OC} = 2\pi m$ where k is the free-space wavenumber, L_{ext} is the length of the VECSEL external cavity, ϕ_{OC} is the output coupler (OC) reflection phase, and $\phi_{MS}(n)$ is the phase of the complex

metasurface reflection coefficient which depends on the refractive index of the QC gain material. If the refractive index of the QC material is tuned, the lasing frequency of the QC-VECSEL must tune in order to maintain a roundtrip phase accumulation that is a multiple of 2π . Using these round-trip expressions, and assuming $\phi_{OC} = \pi$, $\phi_{MS} \approx 0$ (operating near the center of the metasurface resonance), we can write the following expression for the frequency tuning (Δf) in response to a change in refractive index:

$$\frac{\Delta f}{f} = \frac{c}{4\pi f L_{ext}} \frac{d\phi}{dn} \Delta n = \frac{4Q_{MS}\Gamma}{\pi(2m+1)} \frac{\Delta n}{n}$$

Where n is the refractive index of the QC material, Δn is the change in refractive index, f is the operating frequency, Q_{MS} is the quality factor of the metasurface resonance (extracted from simulation), Γ is a near-field metasurface confinement factor (usually close to unity), and $d\phi/dn$ is the rate change of the metasurface phase with refractive index. The second equivalence is made by substituting $L_{ext} = (2m+1)c/4f$, and $d\phi/dn = (d\phi/df)(df/dn) = (4Q_{MS}/f)(\Gamma/f/n)$, assuming a Lorentzian model for the metasurface resonance. This is the same as the tuning expression for a ridge waveguide, scaled by the factor $4Q_{MS}\Gamma/\pi(2m+1)$. Therefore, the tuning coefficient can be larger or smaller than that of a ridge waveguide, depending on the quality factor of the metasurface and the length of the external cavity.

For variations in the external cavity length of the VECSEL, we can start with the round-trip expression and use the same approach to write:

$$\frac{\Delta f}{f} = \frac{\pi(2m)}{\pi(2m+1) + 4Q_{MS}L} \frac{\Delta L}{L}$$

We find the tuning is reduced by either increasing the length of the cavity or increasing the quality factor of the metasurface. The metasurface quality factor can reduce the tuning because the changing phase of the metasurface as the frequency is tuned works to counter the changing cavity length.

ACKNOWLEDGMENT

This work was performed, in part, at the Center for Integrated Nanotechnologies, an Office of Science User Facility operated for the U.S. Department of Energy (DOE) Office of Science. Sandia National Laboratories is a multimission laboratory managed and operated by National Technology and Engineering Solution of Sandia, LLC., a wholly owned subsidiary of Honeywell International, Inc., for the U.S. Department of Energy's National Nuclear Security Administration under contract DE-NA-0003525. The authors would like to thank A. Maestrini, I. Mehdi, J. V. Siles, R. Lin, C. Lee, J. Gill, and G. Chattopadhyay for providing the Schottky diode LO source and mixers.

REFERENCES

[1] B. S. Williams, "Terahertz quantum-cascade lasers," *Nat. Photon.*, vol. 1, no. 9, pp. 517-525, Sep 2007, doi: 10.1038/nphoton.2007.166.
 [2] I. R. Medvedev, C. F. Neese, G. M. Plummer, and F. C. De Lucia, "Submillimeter spectroscopy for chemical analysis with absolute specificity," *Opt. Lett.*, vol. 35, no. 10, pp. 1533-1535, May 2010, doi: 10.1364/Ol.35.001533.

[3] M. Naftaly, N. Vieweg, and A. Deninger, "Industrial Applications of Terahertz Sensing: State of Play," *Sensors-Basel*, vol. 19, no. 19, Oct 2019, doi: 10.3390/s19194203.
 [4] A. J. L. Adam *et al.*, "Beam patterns of terahertz quantum cascade lasers with subwavelength cavity dimensions," *Appl. Phys. Lett.*, vol. 88, no. 15, Apr 2006, doi: 10.1063/1.2194889.
 [5] A. W. M. Lee, B. S. Williams, S. Kumar, Q. Hu, and J. L. Reno, "Tunable terahertz quantum cascade lasers with external gratings," *Opt. Lett.*, vol. 35, no. 7, pp. 910-912, Apr 2010, doi: 10.1364/Ol.35.000910.
 [6] J. Xu *et al.*, "Tunable terahertz quantum cascade lasers with an external cavity," *Appl. Phys. Lett.*, vol. 91, no. 12, Sep 2007, doi: 10.1063/1.2786587.
 [7] H. Richter, N. Rothbart, and H. W. Hubers, "Characterizing the beam properties of terahertz quantum-cascade lasers," *J. Infrared Millim. Terahertz Waves*, vol. 35, no. 8, pp. 686-698, Aug 2014, doi: 10.1007/s10762-014-0084-x.
 [8] L. Y. Xu, C. A. Curwen, D. G. Chen, J. L. Reno, T. Itoh, and B. S. Williams, "Terahertz metasurface quantum-cascade VECSELS: theory and performance," *IEEE J. Sel. Top. Quantum Electron.*, vol. 23, no. 6, p. 1200512, Nov-Dec 2017, doi: 10.1109/Jstqe.2017.2693024.
 [9] L. Y. Xu, C. A. Curwen, P. W. C. Hon, Q. S. Chen, T. Itoh, and B. S. Williams, "Metasurface external cavity laser," *Appl. Phys. Lett.*, vol. 107, no. 22, Nov 2015, doi: 10.1063/1.4936887.
 [10] C. A. Curwen, J. L. Reno, and B. S. Williams, "Broadband continuous single-mode tuning of a short-cavity quantum-cascade VECSEL," *Nat. Photon.*, vol. 13, no. 12, pp. 855-859, Dec 2019, doi: 10.1038/s41566-019-0518-z.
 [11] A. D. Kim, C. A. Curwen, Y. Wu, J. L. Reno, S. J. Addamane, and B. S. Williams, "Wavelength Scaling of Widely-Tunable Terahertz Quantum-Cascade Metasurface Lasers," *IEEE Journal of Microwaves*, vol. 3, pp. 305-318, Jan 2022, doi: 10.1109/jmw.2022.3224640.
 [12] P. Khosropanah *et al.*, "Phase locking of a 2.7 THz quantum cascade laser to a microwave reference," *Opt. Lett.*, vol. 34, no. 19, pp. 2958-2960, Oct 2009, doi: 10.1364/Ol.34.002958.
 [13] D. Rabanus *et al.*, "Phase locking of a 1.5 Terahertz quantum cascade laser and use as a local oscillator in a heterodyne HEB receiver," *Opt. Express*, vol. 17, no. 3, pp. 1159-1168, Feb 2009, doi: 10.1364/Oe.17.001159.
 [14] A. L. Betz, R. T. Boreiko, B. S. Williams, S. Kumar, Q. Hu, and J. L. Reno, "Frequency and phase-lock control of a 3 THz quantum cascade laser," *Opt. Lett.*, vol. 30, no. 14, pp. 1837-1839, Jul 2005, doi: 10.1364/Ol.30.001837.
 [15] A. A. Danylov *et al.*, "Frequency stabilization of a single mode terahertz quantum cascade laser to the kilohertz level," *Opt. Express*, vol. 17, no. 9, pp. 7525-7532, Apr 2009, doi: 10.1364/Oe.17.007525.
 [16] S. Barbieri *et al.*, "Phase-locking of a 2.7-THz quantum cascade laser to a mode-locked erbium-doped fibre laser," *Nat. Photon.*, vol. 4, no. 9, pp. 636-640, Sep 2010, doi: 10.1038/Nphoton.2010.125.
 [17] L. Consolino *et al.*, "Phase-locking to a free-space terahertz comb for metrological-grade terahertz lasers," *Nat Commun*, vol. 3, Sep 2012, doi: 10.1038/ncomms2048.
 [18] M. Ravarolo *et al.*, "Phase-locking of a 2.5 THz quantum cascade laser to a frequency comb using a GaAs photomixer," *Opt. Lett.*, vol. 36, no. 20, pp. 3969-3971, Oct 2011, doi: 10.1364/Ol.36.003969.
 [19] A. Danylov, N. Erickson, A. Light, and J. Waldman, "Phase locking of 2.324 and 2.959 terahertz quantum cascade lasers using a Schottky diode harmonic mixer," *Opt. Lett.*, vol. 40, no. 21, pp. 5090-5092, Nov 2015, doi: 10.1364/Ol.40.005090.
 [20] A. A. Danylov, A. R. Light, J. Waldman, N. R. Erickson, X. F. Qian, and W. D. Goodhue, "2.32 THz quantum cascade laser frequency-locked to the harmonic of a microwave synthesizer source," *Opt. Express*, vol. 20, no. 25, pp. 27908-27914, Dec 2012, doi: 10.1364/Oe.20.027908.
 [21] J. R. Freeman *et al.*, "Injection locking of a terahertz quantum cascade laser to a telecommunications wavelength frequency comb," *Optica*, vol. 4, no. 9, pp. 1059-1064, Sep 2017, doi: 10.1364/Optica.4.001059.
 [22] F. Cappelli *et al.*, "Subkilohertz linewidth room-temperature mid-infrared quantum cascade laser using a molecular sub-Doppler reference," *Opt. Lett.*, vol. 37, no. 23, pp. 4811-4813, Dec 2012, doi: 10.1364/Ol.37.004811.
 [23] Y. Ren *et al.*, "Frequency locking of single-mode 3.5-THz quantum cascade lasers using a gas cell," *Appl. Phys. Lett.*, vol. 100, no. 4, Jan 2012, doi: 10.1063/1.3679620.
 [24] H. Richter *et al.*, "Submegahertz frequency stabilization of a terahertz quantum cascade laser to a molecular absorption line," *Appl. Phys. Lett.*, vol. 96, no. 7, Feb 2010, doi: 10.1063/1.3324703.

- [25] M. I. Amanti, M. Fischer, G. Scalari, M. Beck, and J. Faist, "Low-divergence single-mode terahertz quantum cascade laser," *Nat. Photon.*, vol. 3, no. 10, pp. 586-590, Oct 2009, doi: 10.1038/Nphoton.2009.168.
- [26] C. A. Curwen *et al.*, "Thin THz QCL active regions for improved continuous-wave operating temperature," *AIP Adv.*, vol. 11, no. 12, p. 125018, Dec 2021, doi: 10.1063/5.0071953.
- [27] L. Y. Xu, D. G. Chen, T. Itoh, J. L. Reno, and B. S. Williams, "Focusing metasurface quantum-cascade laser with a near diffraction-limited beam," *Opt. Express*, vol. 24, no. 21, pp. 24117-24128, Oct 2016, doi: 10.1364/Oe.24.024117.
- [28] D. Jayfasankar *et al.*, "A 3.5-THz, x6-Harmonic, Single-Ended Schottky Diode Mixer for Frequency Stabilization of Quantum-Cascade Lasers," *IEEE Trans. Terahertz Sci. Technol.*, vol. 11, no. 6, pp. 684-694, Nov 2021, doi: 10.1109/Tthz.2021.3115730.
- [29] R. Lang and K. Kobayashi, "External Optical Feedback Effects on Semiconductor Injection-Laser Properties," *IEEE J. Quantum Electron.*, vol. 16, no. 3, pp. 347-355, 1980, doi: Doi 10.1109/Jqe.1980.1070479.
- [30] S. Barbieri *et al.*, "Heterodyne mixing of two far-infrared quantum cascade lasers by use of a point-contact Schottky diode," *Opt. Lett.*, vol. 29, no. 14, pp. 1632-1634, Jul 2004, doi: 10.1364/Ol.29.001632.
- [31] A. Barkan *et al.*, "Linewidth and tuning characteristics of terahertz quantum cascade lasers," *Opt. Lett.*, vol. 29, no. 6, pp. 575-577, Mar 2004, doi: 10.1364/Ol.29.000575.
- [32] D. J. Hayton *et al.*, "Phase locking of a 3.4 THz third-order distributed feedback quantum cascade laser using a room-temperature superlattice harmonic mixer," *Appl. Phys. Lett.*, vol. 103, no. 5, Jul 2013, doi: 10.1063/1.4817319.
- [33] A. Maestrini *et al.*, "Design and Characterization of a Room Temperature All-Solid-State Electronic Source Tunable From 2.48 to 2.75 THz," *IEEE Trans. Terahertz Sci. Technol.*, vol. 2, no. 2, pp. 177-185, Mar 2012, doi: 10.1109/Tthz.2012.2183740.
- [34] B. Thomas *et al.*, "A Broadband 835-900-GHz Fundamental Balanced Mixer Based on Monolithic GaAs Membrane Schottky Diodes," *IEEE Trans. Microw. Theory Techn.*, vol. 58, no. 7, pp. 1917-1924, Jul 2010, doi: 10.1109/Tmtt.2010.2050181.
- [35] D. J. Hayton, J. R. Gao, J. W. Kooi, Y. Ren, W. Zhang, and G. de Lange, "Stabilized hot electron bolometer heterodyne receiver at 2.5 THz," *Appl. Phys. Lett.*, vol. 100, no. 8, Feb 2012, doi: 10.1063/1.3688032.
- [36] T. Alam *et al.*, "Frequency and power stabilization of a terahertz quantum-cascade laser using near-infrared optical excitation," *Opt. Express*, vol. 27, no. 25, pp. 36846-36854, Dec 2019, doi: 10.1364/Oe.27.036846.
- [37] B. Wei *et al.*, "Amplitude stabilization and active control of a terahertz quantum cascade laser with a graphene loaded split-ring-resonator array," *Appl. Phys. Lett.*, vol. 112, no. 20, May 2018, doi: 10.1063/1.5027687.
- [38] T. Nakamura, S. Tani, I. Ito, M. Endo, and Y. Kobayashi, "Piezo-electric transducer actuated mirror with a servo bandwidth beyond 500 kHz," *Opt. Express*, vol. 28, no. 11, pp. 16118-16125, May 2020, doi: 10.1364/Oe.390042.

Christopher A Curwen received the B.Sc. degree in Electrical Engineering from Pennsylvania State University in 2012, and M.Sc. and Ph.D. degrees from the University of California, Los Angeles in 2014 and 2019 respectively. He currently working at the Jet Propulsion Lab.

Sadvikas Addamane received the B.S. and Ph.D. degrees in Electrical Engineering from the University of New Mexico, Albuquerque, in 2013 and 2017, respectively. From 2017 to 2019, he was a Post-Doctoral Scholar with the University of New Mexico. In 2019, he became a Post-Doctoral Appointee with Sandia National Laboratories, where he then became a Senior Member of Technical Staff in 2021. His research interests focus on development of epitaxial strategies for growth of novel semiconductor devices including single-photon sources, MWIR and THz lasers, detectors, 2DEGs and saturable absorbers.

Benjamin S. Williams received the Ph.D. degree from the Massachusetts Institute of Technology, Cambridge, Massachusetts in 2003 in Electrical Engineering and Computer Science. He was a Postdoctoral Associate at the Research Laboratory of Electronics at MIT from 2003-2006. In 2007, he joined the Electrical Engineering Department at the University of California, Los Angeles, where he is currently Professor and a Henry Samueli Fellow. His research interests include quantum cascade lasers, intersubband and

intersublevel devices in semiconductor nanostructures, and terahertz metamaterials and plasmonics. He is currently an Associate Editor of IEEE Transactions in Terahertz Science and Technology. Prof. Williams has received awards including the Apker Award from the American Physical Society, the Young Faculty Award from the Defense Advanced Research Projects Agency (DARPA), the Early Career Award from the National Science Foundation (NSF CAREER), and the Presidential Early Career Award for Scientists and Engineers (PECASE).